Published in final edited form as:
Exp Mol Pathol. 2014 October ; 97(2): 305–313. doi:10.1016/j.yexmp.2014.08.006.

The inflammasome in alcoholic hepatitis: its relationship with Mallory-Denk body formation

Yue Peng[a], **Barbara A. French**[a], **Brittany Tillman**[a], **T Morgan**[b], and **Samuel W. French**[a,*]

[a]LABioMed at Harbor UCLA Medical Center, Department of Pathology, Torrance, CA, 90509, USA

[b]VA Medical Center, Department of Medicine, Long Beach, CA, USA

Abstract

Recent studies indicate that the inflammasome activation plays important roles in pathogenesis of alcoholic hepatitis (AH). Nod-like receptor protein 3 (NLRP3) is a key component of the macromolecular complex so called the inflammasome that trigger caspase 1-dependent maturation of the precursors of IL-1β and IL-18 cytokines. It is also known that the adaptor proteins including apoptosis-associated speck-like protein containing CARD (ASC) and the mitochondrial antiviral signaling protein (MAVS) are necessary for NLRP3-dependent inflammasome function. Steatohepatitis frequently includes Mallory-Denk body (MDB) formation. In the case of alcoholic steatohepatitis, MDB formation occurs in 80% of biopsies (French 1981; French 1981). While previous studies have focused on in vitro cell lines and mouse models, we are the first group to investigate inflammasome activation in AH liver biopsy specimen and correlate it with MDB formation. Expression of NOD1, NLRP3, ASC, NAIP, MAVS, Caspase 1, IL-1β, IL-18, and other inflammatory components including IL-6, IL-10, TNF-α, IFN-γ, STAT3, p65 was measured in three to eight formalin-fixed paraffin-embedded AH specimens and control normal liver specimens by immunofluorescence staining and quantified by immunofluorescence intensity. The specimens were double stained with ubiquitin to demonstrate the relationship between inflammasome activation and MDB formation. MAVS, caspase1, IL-18, TNF-α showed increases in expression in AH compared to the controls ($p<0.05$), and NAIP expression markedly increased in AH compared to the controls ($p<0.01$). There was a trend that levels of NLRP3, ASC, caspase1, IL-18, IL-10, and p65 expression correlated with the number of MDBs found in the same field of measurement (correlation coefficients were between 0.62 to 0.93, $p<0.05$). Our results demonstrate the activation of the inflammasome in AH and suggest that MDB could be an indicator of the extent of inflammasome activation.

*Corresponding auther: Samuel W. French.

Conflict of interest statement
The authors declare that there are no conflicts of interest.

Keywords

Inflammasome; Mallory-Denk bodies (MDBs); Alcoholic steatohepatitis; liver disease development

Introduction

Mallory-Denk Bodies (MDBs), which are an intracellular deposition of misfolded protein in ballooned hepatocytes, consist of abnormally phosphorylated, ubiquitylated, and cross-linked keratins or non-keratin K18 and 8, and p62 components (Zatloukal, French et al. 2007; Caldwell, Ikura et al. 2010; Basaranoglu, Turhan et al. 2011; Haybaeck, Stumptner et al. 2012). Ballooning of hepatocytes is induced by oxidative stress, and both ballooning of hepatocytes and MDBs are two characteristics of ongoing inflammation (Basaranoglu, Turhan et al. 2011). MDBs are prevalent in various hepatic diseases including the hepatitis B and C viral infection, alcoholic hepatitis (AH), non-alcoholic steatohepatitis, drug injuries and hepatocellular carcinoma (Zatloukal, French et al. 2007; Basaranoglu, Turhan et al. 2011). Although three new mechanisms of MDB formation have been indentified (French, Bardag-Gorce et al. 2010), the molecular mechanism involved in the formation of MDB aggresomes is still not fully understood. Most recently, MDB formation has been shown to occur as the result of the accumulation of undigested protein due to failure of protein quality control mechanisms by the liver cells (Liu, Li et al. 2014).

Inflammasomes are intracellular macromolecular complexes that sense danger signals including infection and metabolic dysregulation, via NOD-like receptors (Martinon, Burns et al. 2002). Among NLRs, NLRP3 is proved to be the major immune sensor to initiate subsequent responses (Kauppinen, Niskanen et al. 2012), the so called NLRP3 inflammasome. Upon activation, NLRP3, in the presence of adapter proteins, such as the apoptosis-associated speck like CARD-domain containing protein (ASC), forms a complex with the effector molecule, pro-caspase-1, which leads to auto-activation of the inactive pro-caspase-1 to form the active caspase-1 (Agostini, Martinon et al. 2004). Caspase-1 subsequently cleaves pro-IL-1β and pro-IL-18 into their mature forms (Cerretti, Kozlosky et al. 1992). IL-1β, a pro-inflammatory cytokine, plays a central role in the inflammation responses. IL-18 activates natural killer cells to produce IFN-γ (Kalina, Kauschat et al. 2000). IL-1β and IL-18 are responsible for the induction of pyroptosis, a pro-inflammatory form of cell death (Lage, Longo et al. 2014).

The cellular localization of inflammasome formation remains controversial (Subramanian, Natarajan et al. 2013). Earlier studies believed that the assembly of the inflammasome occurs in the cytosol since NLRP3 and ASC are cytosolic proteins. A new adaptor protein, mitochondrial antiviral signaling protein (MAVS) has recently been demonstrated in an in vitro study to recruit the inflammasome complex to mitochondrial membrane to further optimize NLRP3 inflammasome activation in generating bioactive IL-1β and IL-18 (Subramanian, Natarajan et al. 2013). This new finding demonstrated a role for mitochondria as platforms integrating multiple innate signaling pathways.

Inflammasomes have been proposed to be triggered in different liver diseases, including drug-induced liver injury, ischemia-reperfusion, endotoxin-induced liver injury and cholestasis, alcoholic and non-alcoholic steatohepatitis, HBV and HCV viral hepatitis, liver fibrosis, autoimmune hepatitis, and so on (Szabo and Csak 2012). To date, all studies about inflammasome activation in AH have been only performed in vitro and in alcohol induced animal models (Szabo and Csak 2012), but not in humans. Inflammasome components including NLRP3, ASC, pro-caspase-1 and mature IL-1β were shown to be upregulated in the liver (Petrasek, Bala et al. 2012), suggesting that inflammasome activation is a component of the liver pathophysiology in AH. To our knowledge, we are the first group to demonstrate inflammasome activation using formalin-fixed paraffin-embedded (FFPE) AH specimens, and investigate its relationship with MDB formation. The current study further deepened our knowledge about mechanisms of MDB formation.

Materials and Methods

Clinical specimens

Human archived FFPE liver biopsies from patients who had AH were obtained from Harbor UCLA hospital archives. In all the cases, MDBs were present per IHC assay in various abundance except in the normal control livers. From three to eight AH specimens and at least three control normal liver specimens were used in this study.

Immunohistochemical staining

FFPE liver biopsy tissue slides were double stained for ubiquitin (Millipore, Temecula, CA) and the second protein as listed in Table 1. Ubiquitin was detected using the second antibody donkey anti-mouse Alexa Fluor 594 (Jackson Labs, West Grove, PA), while the other protein was detected using the second antibody donkey anti-rabbit Alexa Fluor 488 or donkey anti-mouse Alexa Fluor 488 (Jackson Labs, West Grove, PA). All slides were stained with the nuclear stain DAPI (Molecular Probes, Eugene, OR). The fluorescence intensity of staining of the protein of interest was measured quantitatively using 40x objective magnification and a standard exposure time of 800 ms using a Nikon 400 fluorescent microscope with three filters (FITC-green, Texas-red, and tricolor), and the Nikon morphometric system. The results were displayed as a graph attached to the immunofluorescent photography using a screen snip. The staining was compared among MDB forming AH hepatocytes, neighboring non-MDB forming AH hepatocytes, and control normal hepatocytes.

Statistical analysis

All data were presented as the mean ± S.D.. Statistical differences were calculated, and unpaired, two-tailed student's *t*-test was used to compare two groups' variance. Correlation coefficient (r) was calculated between the fluorescent intensity and the abundance of MDB. In general, a *p* value less than 0.05 denoted statistical significance.

Results

Selective inflammasome components were upregulated in AH livers

To date, no studies have been done in human liver specimen to prove that inflammasome is indeed triggered in liver pathogenesis. To particularly investigate if inflammasome activation occurs in AH in vivo and its association with MDB formation, we stained FFPE biopsy specimens with wide spectrum of inflammasome components, including NLRP3, NOD1, NAIP, MAVS, ASC, caspase-1, IL-1β, IL-18, and co-stained with ubiquitin to identify MDBs. The staining is quantified and compared between AH and control livers by immunefluorescence intensity. The intensity measurements and photographs were always taken using the same exposure setting and the same magnification so as to compare the fluorescence intensity of different specimens. MDBs were identified in three high power fields in each AH specimen, and counted as average number per high power field for each specimen. Fluorescence intensity of MDB forming cells of each AH specimen was recorded by averaging measurements in all three high power fields. Fluorescence intensity of neighboring non-MDB forming cells of each AH specimen was recorded by averaging at least 30 measurements in the same three high power fields as above. Fluorescence intensity of each control liver was counted in the same way except that no MDB forming cells were present. The statistic analysis was done based on measurements of three to eight AH livers and three control livers.

Figure 1A shows representative pictures of NLRP3 staining in two AH livers and two control livers. Red fluorescence-labeled MDB (the second column) was demonstrated as a protein aggregation in the cytoplasm, which was present in AH livers but not in control livers. Green fluorescence-labeled NLRP3 (the first column) was demonstrated as a cytoplasmic staining in controls and AH livers, and appeared to co-localize with MDBs, shown in a yellow color with the Tri-Color filter (the third column). The fourth column demonstrated the fluorescence intensity measurement of NLRP3 staining in MDB forming AH cells, in the neighboring non-MDB forming AH cells and in control liver cells. The cells of interest were traced by the yellow line, and fluorescence intensity of the particular spot was measured and recorded. As summarized in figure 1B, comparing with controls, we did not observe statistically significant upregulation of NLRP3 in AH livers. The presence of MDBs did not change levels of NLRP3 expression significantly, although it might alter the cellular distribution of the protein.

In addition to NLRP3 inflammasome, there are NLRP1, NLRC4, and AIM2 inflammasomes which are the four main prototypes of inflammsomes that have been characterized to date (Szabo and Csak 2012). Four inflammsome systems sense different stimulators, but all react through the caspase-1 and the downstream pathway. Neuronal apoptosis inhibitory protein (NAIP) is another NOD like receptor that promotes the assembly and activation of NLRC4 inflammasome. We were therefore interested in studying its expression in AH livers. As shown in Figure 2A and summarized in Figure 2B, NAIP was indeed statistically significantly upregulated in AH livers compared to control livers ($p<0.01$), but its expression was not exclusively co-localized in cells where MDBs formed. Murine NAIPs were reported to interact with the bacterial flagellin or type III secretion system (T3SS) rod components

(Vinzing, Eitel et al. 2008; Miao, Mao et al. 2010), and human NAIP was shown to recognize the T3SS needle subunit (Zhao, Yang et al. 2011). How NAIP is activated in AH livers remains to be determined.

NOD1 and NOD2 proteins are other well characterized NLRs that function as intracellular receptors and induce inflammatory responses through the adapter protein, Rip2 (Travassos, Carneiro et al. 2010). NOD1 was shown to involve sensing of *Chlamydia trachomatis* (Kavathas, Boeras et al. 2013). We investigated NOD1 expression in AH specimens. As shown in Figure 3A and summarized in figure 3B, we did not observe statistically significant upregulation of NOD1 in AH livers comparing to controls. However, there was a trend that NOD1 was recruited to and co-localized with MDBs, so its staining in MDB forming cells was stronger than the neighboring non-MDB forming cells in AH livers ($p<0.05$). This patchy staining pattern was different from that in control livers which was diffuse and uniform. If NOD1 involving inflammasome activation remains to be determined.

ASC and MAVS are both considered as adaptor proteins for inflammasome activation. MAVS is particular interesting, since in vitro study suggested that it was involved in recruitment of inflammasome to mitochondria (Subramanian, Natarajan et al. 2013), which has never been proved in vivo to date. We first demonstrated colocalization of MAVS with mitochondria in human liver biopsies by co-staining MAVS and mitochondria and viewing with a tri-color filter (Figure 4). The yellow color indicated that indeed MAVS is associated with mitochondria in liver biopsy specimens. Furthermore, we did not observe a difference in ASC expression between control livers and AH livers (data not shown). Interestingly, as shown in Figure 5A and summarized in Figure 5B, we observed statistically significant upregulation of MAVS in AH livers comparing to control livers ($p<0.05$), and MAVS expression was not co-localized with MDBs. The separate localization of MAVS (mitochondria associated) and MDB (proteasome associated) was as expected, and proved the specificity of the staining.

To further prove inflammasome activation in AH livers, we compared caspase-1 expression between AH livers and control livers. As shown in Figure 6A and summarized in figure 6B, caspase-1 was indeed upregulated in AH livers ($p<0.05$). The MDB forming cells did not show difference from non-MDB forming cells in expression levels of caspase-1. Moreover, the caspase-1 and the MDBs were not co-localized, as expected.

IL-1β and IL-18 are two downstream cytokines activated upon inflammasome activation. We did not observe statistically significant upregulation of IL-1β in AH livers comparing to control livers (data not shown), but we did observe an upregulation of IL-18 in AH livers (Figure7A and 7B), particularly in MDB forming cells comparing to controls ($p<0.05$), probably due to less variation of IL-18 expression levels in MDB forming cells than that in non-MDB forming cells. This suggests that MDBs are associated with degree of inflammation.

Other inflammatory cytokines were also upregulated in AH livers

We previously demonstrated that both the proinflammatory pathways and growth pathways are activated as a consequence of Toll-like receptor (TLR) signaling, which induce MDB

formation (French, Bardag-Gorce et al. 2010). Moreover, TLR signaling is enhanced by TNF-α and IFN-γ generated by NFκB activation (French, Bardag-Gorce et al. 2010). We therefore used the same method to investigate expression of related inflammatory cytokines and transcription factors involving inflammation including IFN-γ, TNF-α, IL-10, IL-6, STAT3, and p65 in AH livers. Among them, TNF-α showed an upregulation in MDB forming liver cells compared to control liver cells ($p=0.05$) (Figure 8A and Figure 8B), and MDB forming cells tended to have higher levels of TNF-α expression than non-MDB forming cells. Both TNF-α and MDBs appeared to co-localize at the rim of the MDBs. This again suggested that MDB forming hepatocytes are associated with more severe inflammation. We did not detect significant upregulation of other cytokines, likely due to variable disease severity and variable MDB abundance among specimens, as discussed below.

MDBs are indicators of the extent of inflammasome activation

MDB formation is a focal pathological changes in AH livers, and the abundance, the size, and localization of MDBs varied among the FFPE specimens. We hypothesized that MDBs may be associated with different degrees of disease severity, which leads to a wide variation of expression levels of proteins studied and explains statistical insignificance in some staining intensities mentioned above. The average number of MDBs per high power field for each specimen was correlated to the average fluorescence intensity measurement in the same fields for each protein stained. As shown in Table 2, NLRP3, ASC, Caspase-1, IL-18, IL-10, and p65 expression levels were correlated with the abundance of MDBs (correlation coefficients were between 0.62 to 0.93, $p<0.05$), suggesting that amount of MDB formation is an indicator of the severity of inflammasome activation.

Discussion

Emerging evidence has shown that cytosolic NLRs are associated with human diseases including infections, cancer, aging, autoimmune, and inflammatory disorders. Therefore, they are being considered as master regulators of inflammation and cancer (Saxena and Yeretssian 2014). Upon activation, some NLRs form inflammasomes, while others coordinate caspase-independent NF-κB and mitogen activated protein kinase (MAPK) signaling (Saxena and Yeretssian 2014). Moreover, NLRs and their downstream signaling components engage in an intricate crosstalk with cell death and autophagy pathways. Therefore, aberrant NLR signaling which leads to chronic inflammation plays a central role in aging and carcinogenesis (Saxena and Yeretssian 2014).

Animal studies done in IL-1 receptor antagonist treated mice and caspase-1 or ASC or type I IL-1 receptor (IL-1R1) deficient mice (Petrasek, Bala et al. 2012) demonstrated the upregulation of proinflammatory cytokines, including IL-1β, a downstream cytokine of NLR signaling, is a crucial mechanism of hepatopathogenesis of alcoholic liver disease. Their findings also suggested a potential role of IL-1R1 inhibition in the treatment of AH (Petrasek, Bala et al. 2012). The pathogenic role of IL-1β was attributed to the activation of the inflammasome and TLR4-dependent inflammatory signaling only in liver immune cells but not in primary hepatocytes (Csak, Ganz et al. 2011; Petrasek, Bala et al. 2012).

Increased serum levels of IL-1β were observed in patients with ASH (Tilg, Wilmer et al. 1992). However, there is no direct data proving the inflammasome activation in liver specimens from patients with ASH to date.

In the current study, we observed that the inflammasomes were activated in AH, as demonstrated by increased expression of the inflammasome components including NAIP (Fig. 2), MAVS (Fig. 5), caspase-1 (Fig. 6), and IL-18 (Fig. 7) in the FFPE liver biopsies. The immunofluorescence intensity was measured in primary hepatocytes, which may explain why we did not observe upregulation of IL-1β in the specimens. The results indicate that parenchyma cells such as primary hepatocytes do mount inflammatory responses to pathogens by recruitment of mitochondria and activation of the inflammasome complex. Interestingly, we did not observe NRLP3 upregulation (Fig.1) but rather NAIP was upregulated. They are associated with two different inflammasomes. Novel roles have been described for NAIP/NLRC4 inflammasomes, such as phagosomal maturation, activation of inducible nitric oxide synthase, regulation of autophagy, secretion of inflammatory mediators, antibody production, activation of T cells, and others (Lage, Longo et al. 2014). How alcohol consumption connects to NAIP/NLRC4 activation remains to be determined.

Conclusion

We were the first group to report that MDB formation occurs in 80% of AH liver biopsy specimens (French 1981). Several mechanisms have been proposed in the pathogenesis of MDBs (French, Bardag-Gorce et al. 2010). We recently demonstrated that up regulation of the MyD88-dependent TLR4/NFκB pathway in AH where MDBs formed (Liu, Li et al. 2014) using FFPE liver biopsy specimens. As shown in Table 2, expression levels of selective inflammasome components such as NLRP3, ASC, caspase-1, IL-18 correlated with the abundance of MDB present in the specimens with statistically significant correlation coefficients. The results deepen our knowledge about the mechanism of MDB formation and suggest that MDB could be an indicator of the extent of inflammasome activation in AH hepatocytes.

Acknowledgments

This work was supported by the NIH grant (AAU01021898-02) and p50-11999, Morphology Core.

Abbreviations

AH	alcoholic hepatitis
FFPE	formalin-fixed, paraffin-embedded
MDB	Mallory-Denk body
NLRP3	NOD-like receptor protein 3
IL	interleukin
MAVS	mitochondrial antiviral signaling protein

ASC	apoptosis-associated speck-like protein containing a caspase recruitment domain
NAIP	neuronal apoptosis inhibitory protein
TNF-α	tumor necrosis factor α
IFN-γ	interferon γ
NOD1	Nucleotide-binding oligomerization domain-containing protein 1.
STAT3	Signal transducer and activator of transcription 3

References

Agostini L, Martinon F, et al. NALP3 forms an IL-1beta-processing inflammasome with increased activity in Muckle-Wells autoinflammatory disorder. Immunity. 2004; 20(3):319–325. [PubMed: 15030775]

Basaranoglu M, Turhan N, et al. Mallory-Denk Bodies in chronic hepatitis. World J Gastroenterol. 2011; 17(17):2172–2177. [PubMed: 21633525]

Caldwell S, Ikura Y, et al. Hepatocellular ballooning in NASH. J Hepatol. 2010; 53(4):719–723. [PubMed: 20624660]

Cerretti DP, Kozlosky CJ, et al. Molecular cloning of the interleukin-1 beta converting enzyme. Science. 1992; 256(5053):5097–100.

Csak T, Ganz M, et al. Fatty acid and endotoxin activate inflammasomes in mouse hepatocytes that release danger signals to stimulate immune cells. Hepatology. 2011; 54(1):133–144. [PubMed: 21488066]

French SW. The Mallory body: structure, composition, and pathogenesis. Hepatology. 1981; 1(1):76–83. [PubMed: 6269976]

French SW. Nature, pathogenesis and significance of the Mallory body. Semin Liver Dis. 1981; 1(3): 217–231. [PubMed: 7051303]

French SW, Bardag-Gorce F, et al. Mallory-Denk body pathogenesis revisited. World J Hepatol. 2010; 2(8):295–301. [PubMed: 21161012]

Haybaeck J, Stumptner C, et al. Genetic background effects of keratin 8 and 18 in a DDC-induced hepatotoxicity and Mallory-Denk body formation mouse model. Lab Invest. 2012; 92(6):857–867. [PubMed: 22449798]

Kalina U, Kauschat D, et al. IL-18 activates STAT3 in the natural killer cell line 92, augments cytotoxic activity, and mediates IFN-gamma production by the stress kinase p38 and by the extracellular regulated kinases p44erk-1 and p42erk-21. J Immunol. 2000; 165(3):1307–1313. [PubMed: 10903731]

Kauppinen A, Niskanen H, et al. Oxidative stress activates NLRP3 inflammasomes in ARPE-19 cells--implications for age-related macular degeneration (AMD). Immunol Lett. 2012; 147(1–2):29–33. [PubMed: 22698681]

Kavathas PB, Boeras CM, et al. Nod1, but not the ASC inflammasome, contributes to induction of IL-1beta secretion in human trophoblasts after sensing of Chlamydia trachomatis. Mucosal Immunol. 2013; 6(2):235–243. [PubMed: 22763410]

Lage SL, Longo C, et al. Emerging Concepts about NAIP/NLRC4 Inflammasomes. Front Immunol. 2014; 5:309. [PubMed: 25071770]

Liu H, Li J, et al. TLR3/4 Signaling is Mediated via the NFkappaB-CXCR4/7 Pathway in Human Alcoholic Hepatitis and Non Alcoholic Steatohepatitis Which Formed Mallory-Denk Bodies. Exp Mol Pathol. 2014

Liu H, L J. Ufmylation and FATylation pathways are downregulated in human alcoholic and nonalcoholic steatohepatitis, and mice fed DDC, where Mallory-Denk bodies (MDBs) form. Exp Mol Pathol. 2014; 97(1):81–88. [PubMed: 24893112]

Martinon F, Burns K, et al. The inflammasome: a molecular platform triggering activation of inflammatory caspases and processing of proIL-beta. Mol Cell. 2002; 10(2):417–426. [PubMed: 12191486]

Miao EA, Mao DP, et al. Innate immune detection of the type III secretion apparatus through the NLRC4 inflammasome. Proc Natl Acad Sci U S A. 2010; 107(7):3076–3080. [PubMed: 20133635]

Petrasek J, Bala S, et al. IL<-1 receptor antagonist ameliorates inflammasome-dependent alcoholic steatohepatitis in mice. J Clin Invest. 2012; 122(10):3476–3489. [PubMed: 22945633]

Saxena M, Yeretssian G. NOD-Like Receptors: Master Regulators of Inflammation and Cancer. Front Immunol. 2014; 5:327. [PubMed: 25071785]

Subramanian N, Natarajan K, et al. The adaptor MAVS promotes NLRP3 mitochondrial localization and inflammasome activation. Cell. 2013; 153(2):348–361. [PubMed: 23582325]

Szabo G, Csak T. Inflammasomes in liver diseases. J Hepatol. 2012; 57(3):642–654. [PubMed: 22634126]

Tilg H, Wilmer A, et al. Serum levels of cytokines in chronic liver diseases. Gastroenterology. 1992; 103(1):264–274. [PubMed: 1612333]

Travassos LH, Carneiro LA, et al. Nod1 and Nod2 direct autophagy by recruiting ATG16L1 to the plasma membrane at the site of bacterial entry. Nat Immunol. 2010; 11(1):55–62. [PubMed: 19898471]

Vinzing M, Eitel J, et al. NAIP and Ipaf control Legionella pneumophila replication in human cells. J Immunol. 2008; 180(10):6808–6815. [PubMed: 18453601]

Zatloukal K, French SW, et al. From Mallory to Mallory-Denk bodies: what, how and why? Exp Cell Res. 2007; 313(10):2033–2049. [PubMed: 17531973]

Zhao Y, Yang J, et al. The NLRC4 inflammasome receptors for bacterial flagellin and type III secretion apparatus. Nature. 2011; 477(7366):596–600. [PubMed: 21918512]

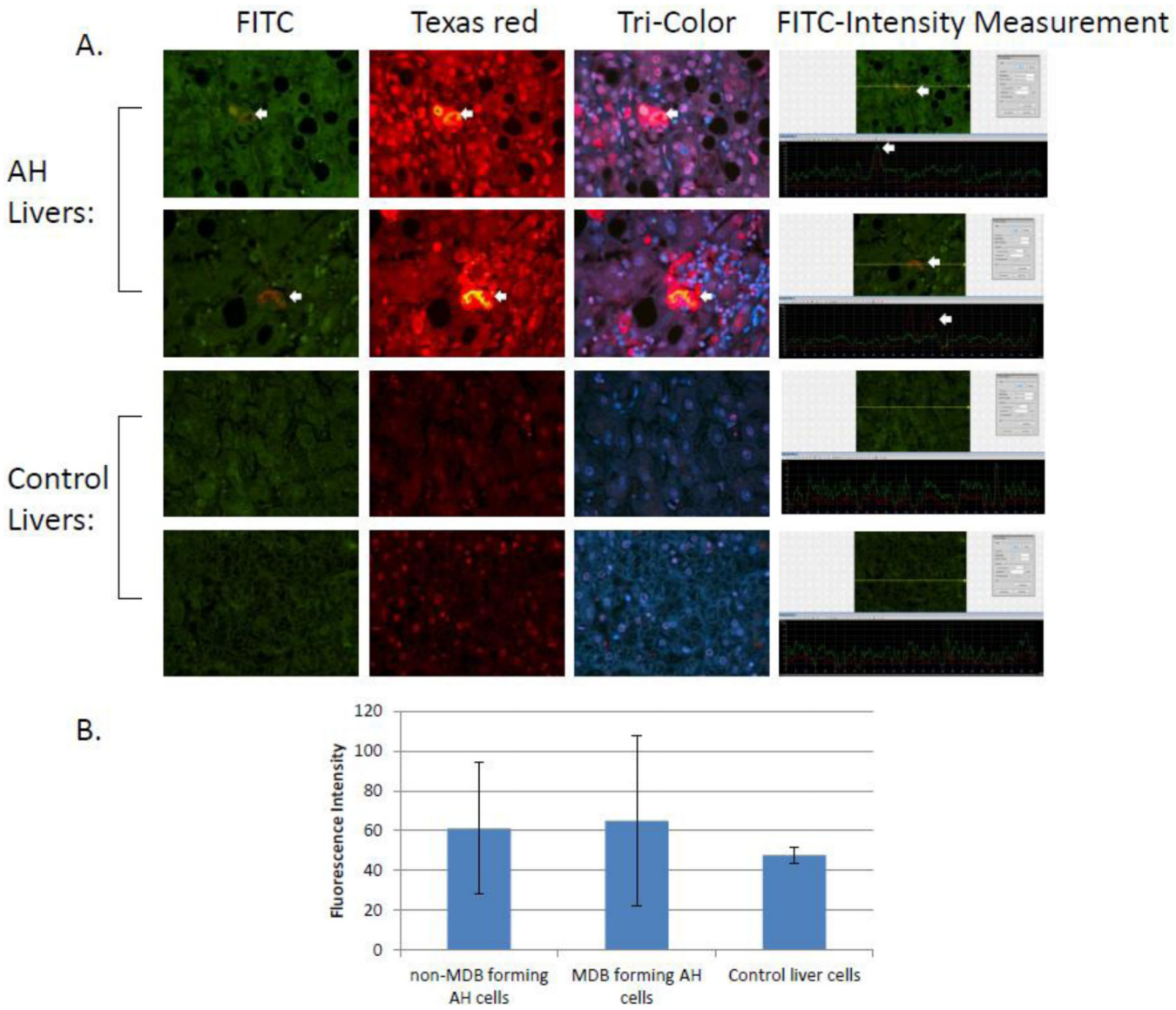

Figure 1. NLRP3 was co-localized with MDBs in AH livers

A. Immunohistochemical analysis of liver biopsies obtained from two representative patients with alcoholic hepatitis and two representative control patients. The specimens were stained for the presence of NLRP3 (green, the first column) and ubiquitin (red, the second column). The arrows point to the MDBs. Note that the MDBs stain both red for ubiquitin and green for NLRP3, shown as yellow color with a tri-color filter (the third column). The round black holes are macrovesicular fat globules in the hepatocytes. The fourth column demonstrated the fluorescence intensity measurement of NLRP3 stain. Screen snips were obtained from the morphometric screen to visualize and compare the intensity of staining in MDB forming hepatocytes, neighboring non-MDB forming cells, and control cells. The fluorescence intensity was traced along the yellow line in the top picture and shown as a green tracer in the bottom picture. B) Fluorescent intensity bar graph of MDB forming hepatocytes, non-

MDB forming hepatocytes, and control cells from three AH specimens and three control specimens. The results were shown as Mean ±S.D.

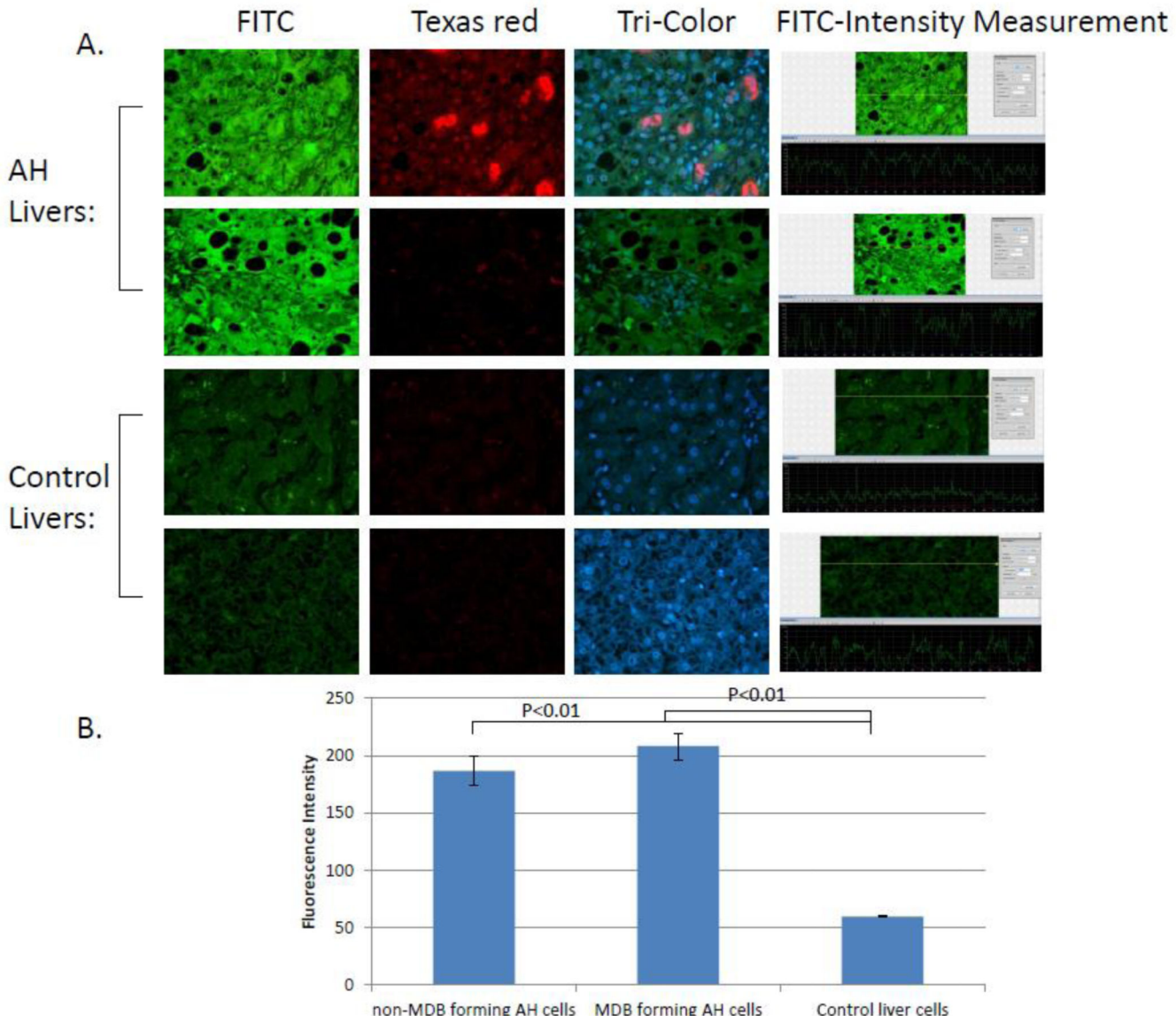

Figure 2. NAIP was up-regulated in AH livers

A. Immunohistochemical analysis of liver biopsies obtained from two representative patients with alcoholic hepatitis and two representative control patients. The specimens were stained for the presence of NAIP (green, the first column) and ubiquitin (red, the second column). There was no co-localization seen with the tri-color filter (the third column). The fourth column demonstrated the fluorescence intensity measurement of NAIP stain. Screen snips were obtained from the morphometric screen to visualize and compare the intensity of staining in MDB forming hepatocytes, neighboring non-MDB forming cells, and control cells. The fluorescence intensity was traced along the yellow line in the top picture and shown as a green tracer in the bottom picture. B) Fluorescent intensity bar graph of MDB forming hepatocytes, non-MDB forming hepatocytes, and control cells from three AH specimens and three control specimens. The results were shown as Mean ±S.D.. The comparisons showing statistical significance ($p<0.01$) were indicated.

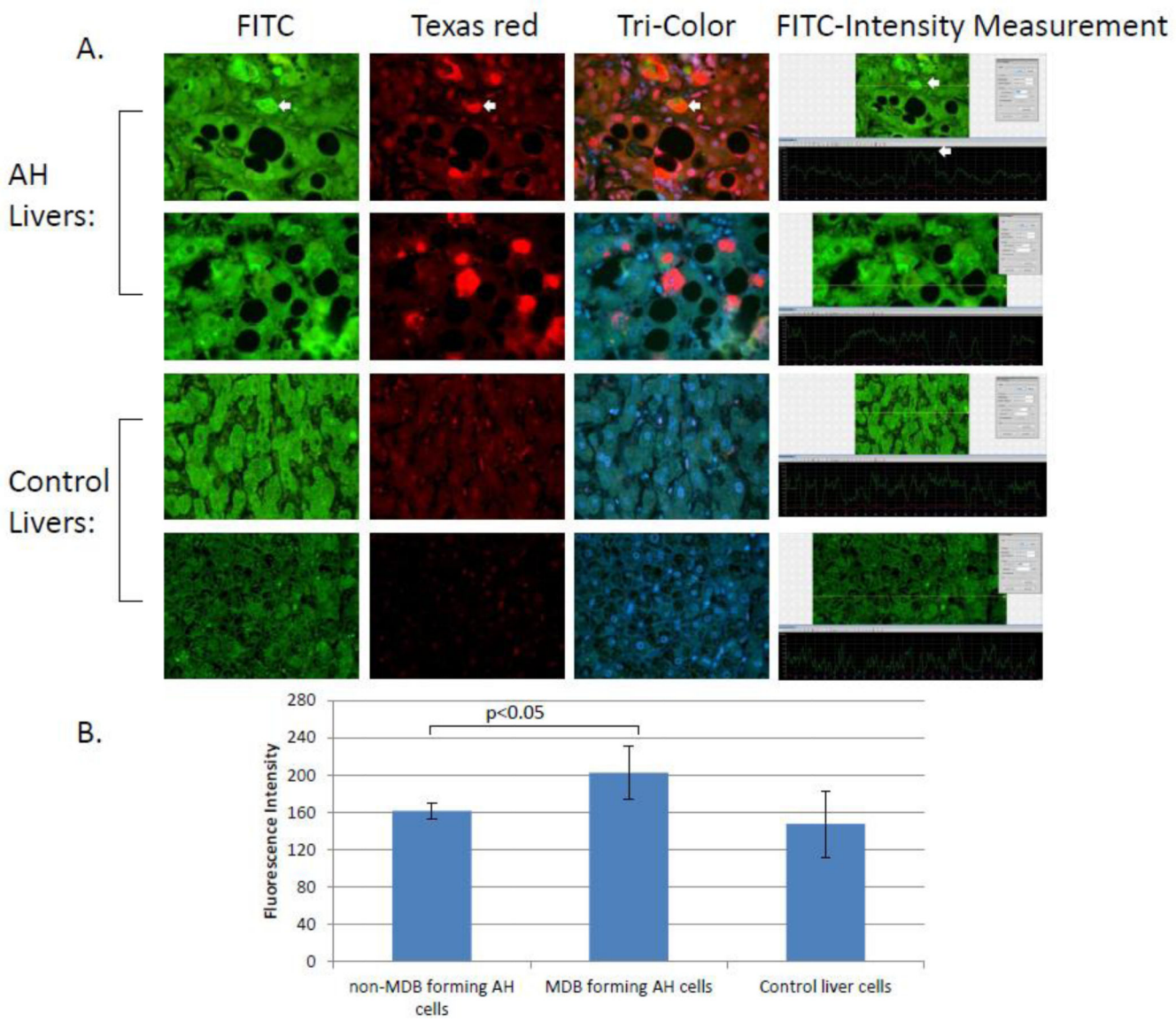

Figure 3. NOD1 was co-localized with MDBs in AH livers

A. Immunohistochemical analysis of liver biopsies obtained from two representative patients with alcoholic hepatitis and two representative control patients. The specimens were stained for the presence of NOD1 (green, the first column) and ubiquitin (red, the second column). The arrows point to the MDBs. The yellow fringe on the MDB indicates colocalization of both proteins at the rim of the MDBs (the third column). The fourth column demonstrated the fluorescence intensity measurement of NOD1 stain. Screen snips were obtained from the morphometric screen to visualize and compare the intensity of staining in MDB forming hepatocytes, neighboring non-MDB forming cells, and control cells. The fluorescence intensity was traced along the yellow line in the top picture and shown as a green tracer in the bottom picture. B) Fluorescent intensity bar graph of MDB forming hepatocytes, non-MDB forming hepatocytes, and control cells from three AH specimens and three control

specimens. The results were shown as Mean ±S.D.. The comparison showing statistical significance ($p<0.05$) was indicated.

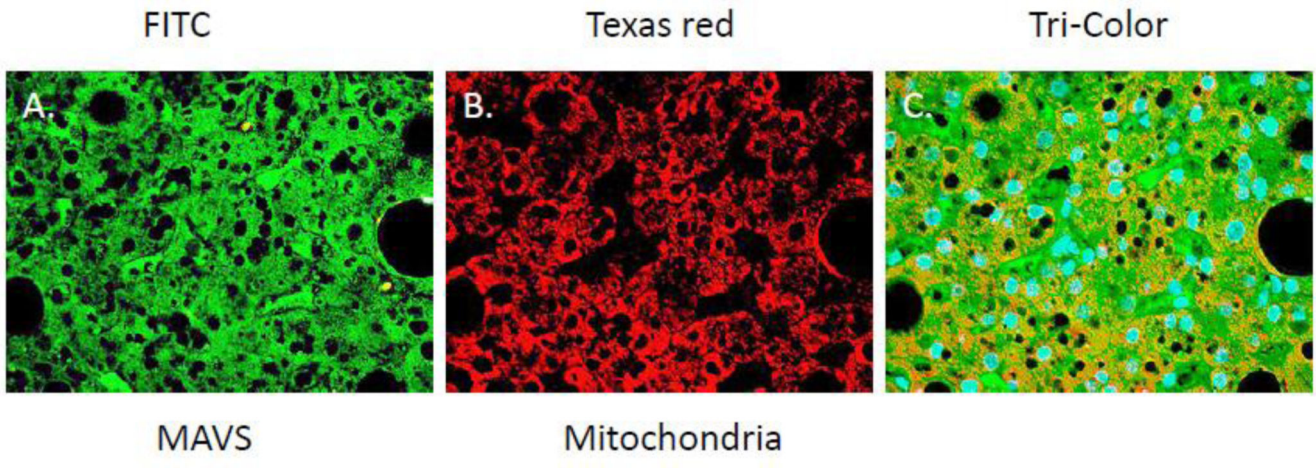

Figure 4. MAVS was co-localized with mitochondria in hepatocytes in vivo

Immunohistochemical analysis of a liver biopsy from a representative patient with AH. The specimen was co-stained for the presence of MAVS (A) and mitochondria (B), and viewed with the FITC filter, the Texas-red filter, or the Tri-color filter. The yellow color in (C) indicates the co-localization of MAVS with mitochondria.

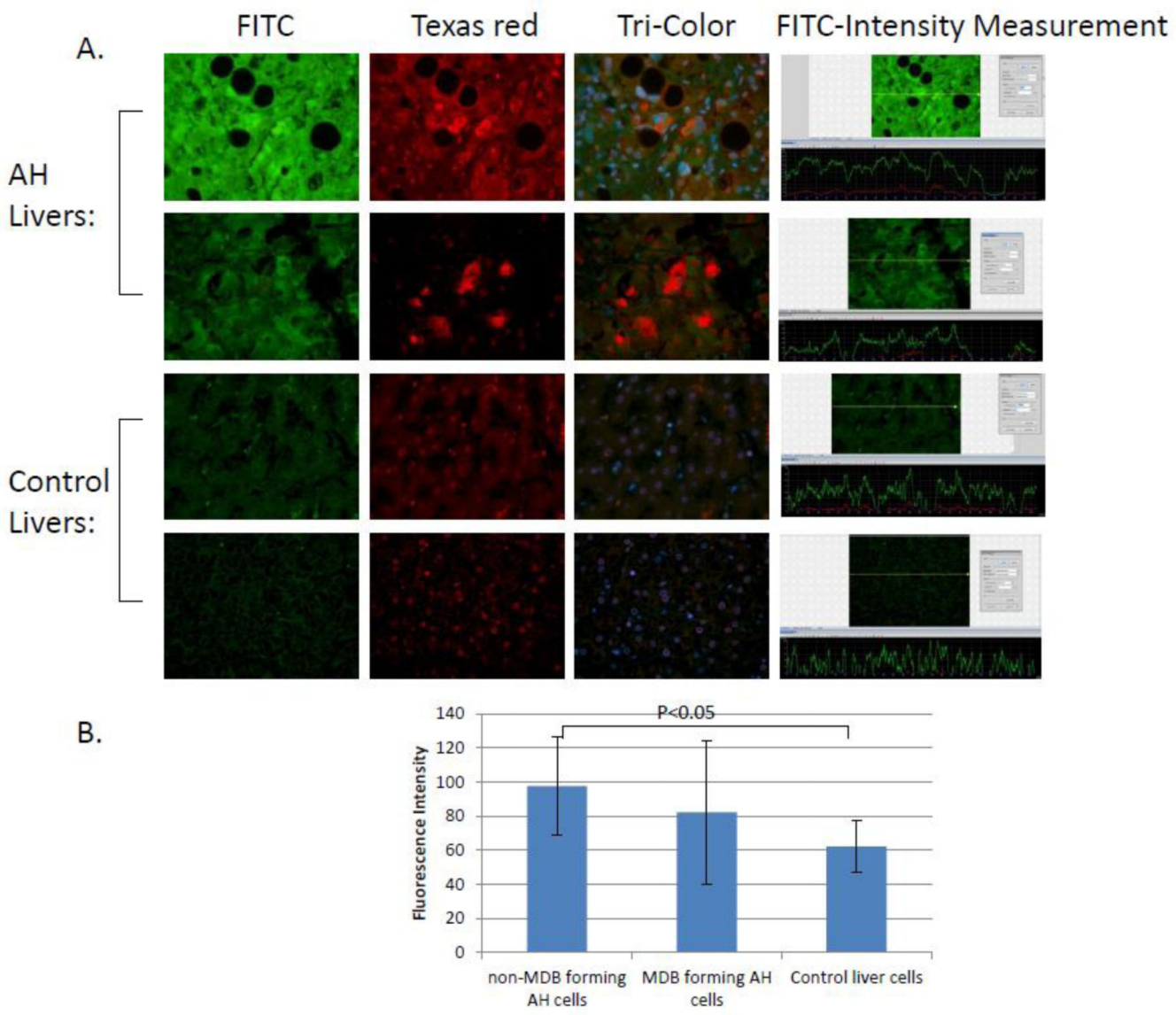

Figure 5. MAVS was up-regulated in AH livers

A. Immunohistochemical analysis of liver biopsies obtained from two representative patients with alcoholic hepatitis and two representative control patients. The specimens were stained for the presence of MAVS (green, the first column) and ubiquitin (red, the second column). There was no co-localization seen with the tri-color filter (the third column). The fourth column demonstrated the fluorescence intensity measurement of the MAVS stain. Screen snips were obtained from the morphometric screen to visualize and compare the intensity of staining in MDB forming hepatocytes, neighboring non-MDB forming cells, and control cells. The fluorescence intensity was traced along the yellow line in the top picture and shown as a green tracer in the bottom picture. B) Fluorescent intensity bar graph of MDB forming hepatocytes, non-MDB forming hepatocytes, and control cells from eight AH specimens and four control specimens. The results were shown as Mean ±S.D.. The comparison showing statistical significance ($p<0.05$) was indicated.

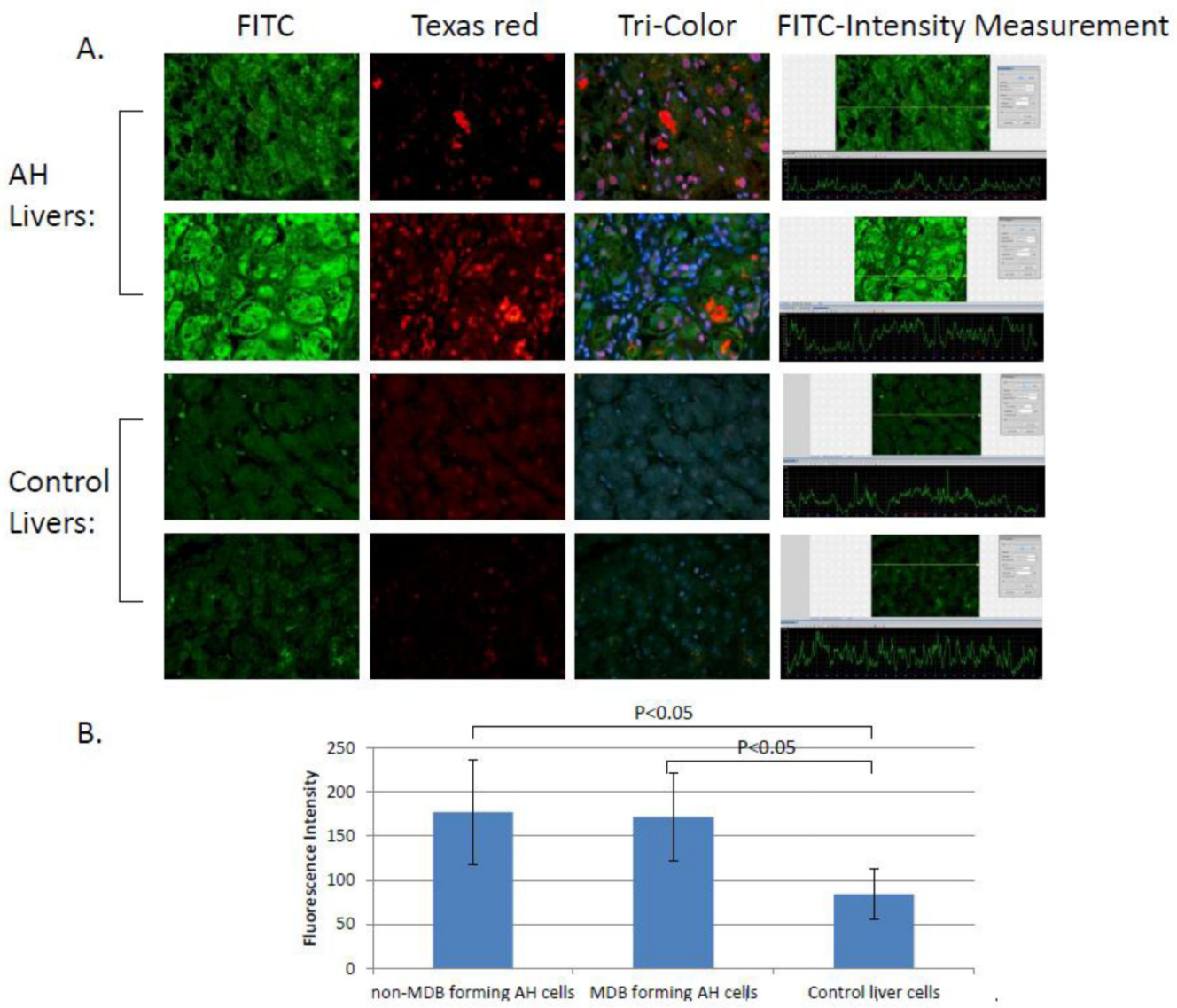

Figure 6. Caspase-1 was up-regulated in AH livers

A. Immunohistochemical analysis of liver biopsies obtained from two representative patients with alcoholic hepatitis and two representative control patients. The specimens were stained for the presence of caspase-1 (green, the first column) and ubiquitin (red, the second column). There was no co-localization seen with the tri-color filter (the third column). The fourth column demonstrated the fluorescence intensity measurement of caspase-1 stain. Screen snips were obtained from the morphometric screen to visualize and compare the intensity of staining in MDB forming hepatocytes, neighboring non-MDB forming cells, and control cells. The fluorescence intensity was traced along the yellow line in the top picture and shown as a green tracer in the bottom picture. B) Fluorescent intensity bar graph of MDB forming hepatocytes, non-MDB forming hepatocytes, and control cells from seven AH specimens and three control specimens. The results were shown as Mean ±S.D.. The comparisons showing statistical significance ($p<0.05$) were indicated.

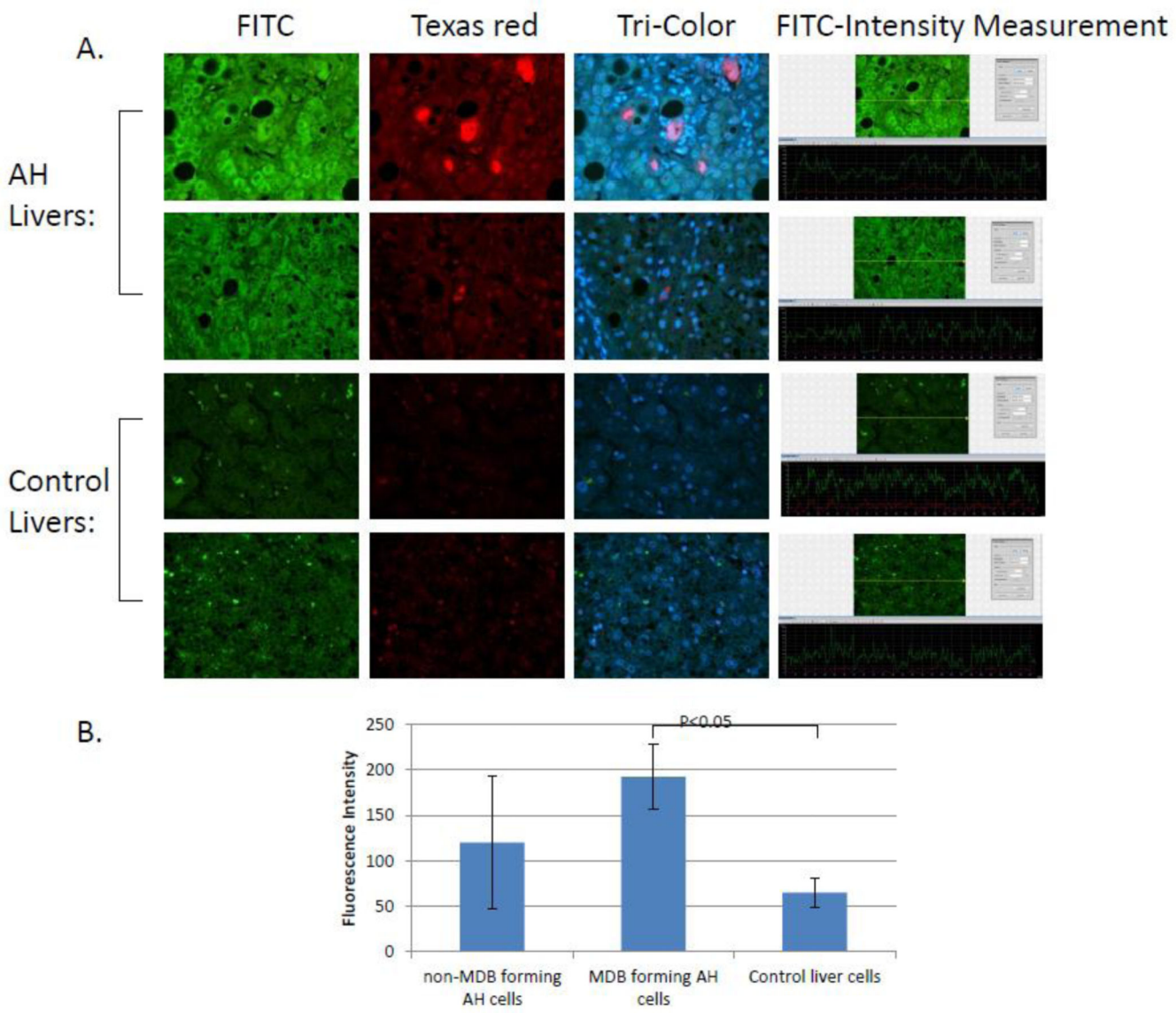

Figure 7. IL-18 was up-regulated in AH livers

A. Immunohistochemical analysis of liver biopsies obtained from two representative patients with alcoholic hepatitis and two representative control patients. The specimens were stained for the presence of IL-18 (green, the first column) and ubiquitin (red, the second column). The fourth column demonstrated the fluorescence intensity measurement of IL-18 stain. Screen snips were obtained from the morphometric screen to visualize and compare the intensity of staining in MDB forming hepatocytes, neighboring non-MDB forming cells, and control cells. The fluorescence intensity was traced along the yellow line in the top picture and shown as a green tracer in the bottom picture. B) Fluorescent intensity bar graph of MDB forming hepatocytes, non-MDB forming hepatocytes, and control cells from three AH specimens and three control specimens. The results were shown as Mean ±S.D.. The comparison showing statistical significance ($p<0.05$) was indicated.

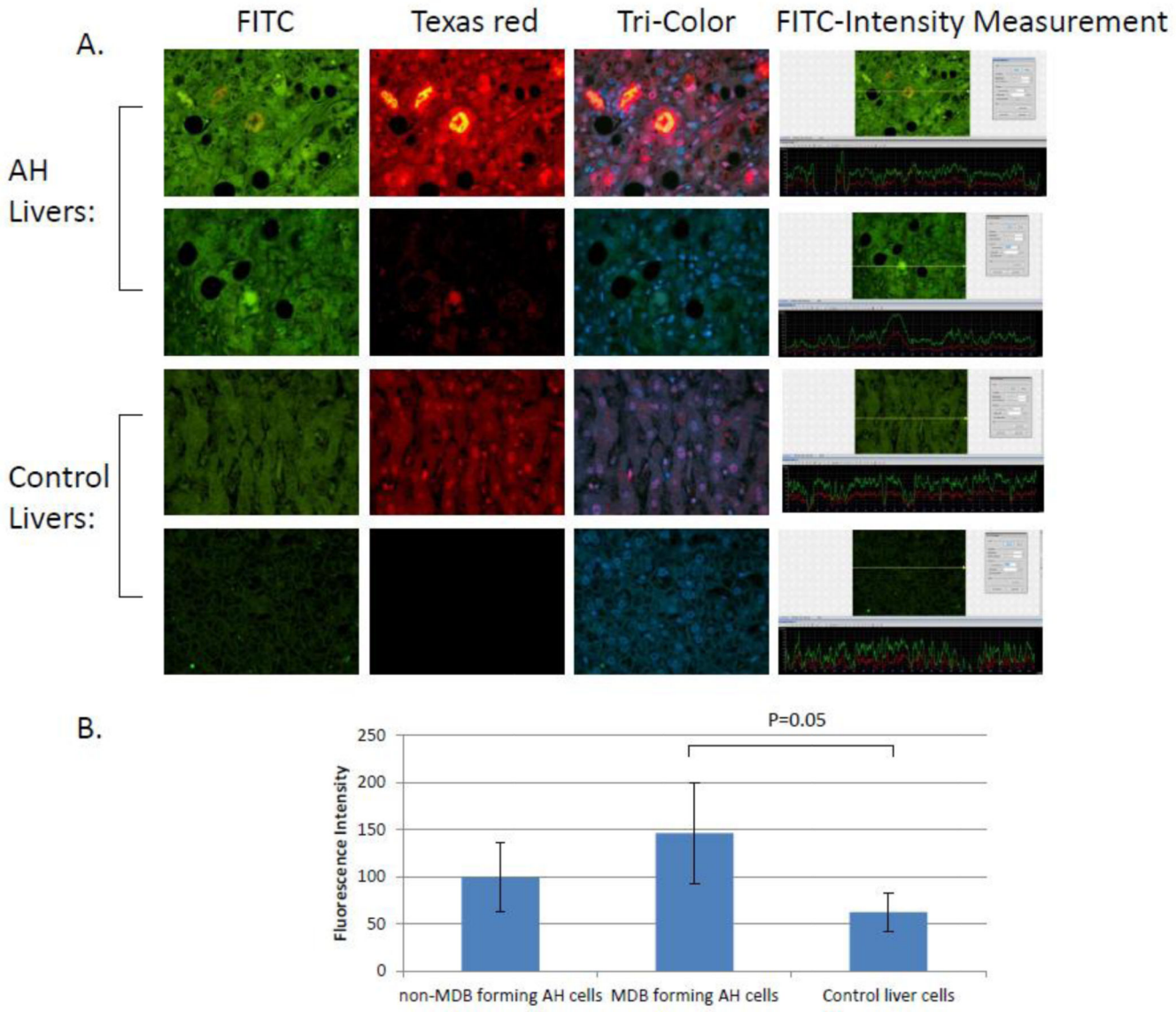

Figure 8. TNF-α was slightly up-regulated in AH livers and co-localized with MDBs

A. Immunohistochemical analysis of liver biopsies obtained from two representative patients with alcoholic hepatitis and two representative control patients. The specimens were stained for the presence of TNF-α (green, the first column) and ubiquitin (red, the second column). Note that the MDBs stain both red for ubiquitin and green for TNF-α, shown as yellow color with a tri-color filter (the third column). This indicates that TNF-α protein is present within the aggresome (MDB). The fourth column demonstrated the fluorescence intensity measurement of TNF-α stain. Screen snips were obtained from the morphometric screen to visualize and compare the intensity of staining in MDB forming hepatocytes, neighboring non-MDB forming cells, and control cells. The fluorescence intensity was traced along the yellow line in the top picture and shown as a green tracer in the bottom picture. B) Fluorescent intensity bar graph of MDB forming hepatocytes, non-MDB forming

hepatocytes, and control cells from three AH specimens and three control specimens. The results were shown as Mean ±S.D.. The comparison with p=0.05 was indicated.

Table 1

Antibodies used in the study with animal source and company/vendor

Antibody	Antibody	Type Company/Vendor
NOD-1	Rabbit	Lifespan Biosciences, Seattle, WA
NLRP3	Mouse	Adipogen, San Diego, CA
NAIP	Rabbit	Lifespan Biosciences, Seattle, WA
MAVS	Rabbit	ABCAM, Cambridge, MA ASC Mouse Novus Biologicals, Littleton, CO
Caspase-1	Rabbit	Epitomics, Burlingame, CA
IL-1β	Rabbit	Lifespan Biosciences, Seattle, WA
IL-18	Rabbit	Lifespan Biosciences, Seattle, WA
IFN-γ	Mouse	Millipore, Temecula, CA
TNF-α	Mouse	R&D Systems, Minneapolis, MN
IL-10	Rabbit	ABCAM, Cambridge, MA
IL-6	Mouse	Millipore, Temecula, CA
Stat3	Rabbit	Millipore, Temecula, CA
P65	Mouse	eBioscience, Santa Clara, CA
Mitochondria (MTC02)	Mouse	ABCAM, Cambridge, MA

Table 2

Correlation between amounts of MDB and intensities of staining

Inflammasome and related components	Correlation Coefficient (r)	P value
NLRP3	0.81	<0.05*
NOD1	0.42	>0.05
ASC	0.92	<0.05*
MAVS	0.47	>0.05
Caspase-I	0.62	<0.05*
IL-18	0.92	<0.05*
IL-1 β	−0.29	>0.05
TNF-α	0.76	>0.05
IL-10	0.93	<0.05*
IL-6	0.17	>0.05
Stat3	0.17	>0.05
p65	0.91	<0.05*